Research & Reviews: Journal of Material Sciences
DOI: 10.4172/2321-6212.1000182

e-ISSN: 2321-6212
p-ISSN: 2347-2278

Extremely Low Cycle Fatigue Behaviors of Anti-Seismic Steel HRB400 Reinforcing Steel Bars under Strong Earthquakes

Luo Yun-Rong[1,3], Wang Qing-Yuan[2], Fu Lei[1*], Xie Wen-ling[1] and Zhang Ying-Qian[4]

[1]College of Mechanical Engineering, Sichuan University of Science & Engineering, Zigong, China

[2]Department of Civil Engineering and Mechanics, Sichuan University, Chengdu, China

[3]Key Lab of Material Corrosion and Protection of Sichuan Province, Zigong, China

[4]School of Civil Engineering, Sichuan University of Science and Engineering; Zigong, China

Research Article

Received: 23/06/2017
Accepted: 20/07/2017
Published: 27/07/2017

***For Correspondence**

FU Lei, College of mechanical engineering, Sichuan University of Science & Engineering, Zigong, China,
Tel: +8615808230830.

Email: kunmingfulei@126.com

Keywords: HRB400III steel bar, Extremely low cycle fatigue (ELCF), Life prediction, Micro-fracture mechanism

ABSTRACT

The extremely low cycle fatigue (ELCF) behaviors of anti-seismic steel HRB400 reinforcing steel bars were comprehensively studied following the cyclic push-pull loading tests with extremely high strain amplitudes (up to ±12.8%). The cyclic stress response characteristics and cyclic stress-strain relationships were investigated. The cyclic response characteristics were closely related to the strain amplitudes, and the secondary hardening phenomenon appeared under some strain amplitudes. The strain-life data from the axial tests were used to derive suitable Coffin-Manson parameters for the test material. The scanning electron microscope (SEM) morphology revealed ELCF damage mechanisms were distinctive of those typical from LCF. Compared with the common low-cycle fatigue (LCF) fracture region, several unique features in the ELCF regime can be noticed, including the deviations of the fatigue life from the Coffin-Manson law and the transformation of fatigue cracking modes.

INTRODUCTION

Nowadays, the fatigue properties of steel structures are generally taken into account in structure designs, to predict and prevent possible failure under cyclic loads [1], especially very large-strain cyclic loading, such as strong earthquakes [2]. Under this condition, materials normally fail in very small number of cycles (<100 cycles), and behave differently from common Low Cycle Fatigue (LCF) behaviors. To distinguish this very-low-cycle regime from larger cycle parts of the LCF region, the fatigue failure at very small number of cycles (<100 cycles) is termed as extremely low cycle fatigue (ELCF) [3-8]. Extremely low cycle fatigue, with the fatigue life of less than 100 cycles, is the extremely behaviour of Low Cycle Fatigue (LCF) [1-3]. The alternative stress borne by the material or structure which was damaged in the ELCF greatly exceeded the yield strength.

In recent years, accidents of the structure or facilities in aviation, transportation, petrochemical and construction industries occurred frequently. The analysis of failure suggested that many accidents were caused by the high strain low cycle fatigue behavior of building structure. In some accidents, such as strong earthquakes, buildings experienced low cycle fatigue or extremely low cycle fatigue, where strain amplitude was very high (several times of the yield strain) and the fatigue life was extremely short, sometimes only several cycles [9,10], which caused huge disaster or property damage in an unexpectedly short time. A common life example of ELCF are steel structures failing due to extreme loading conditions caused by strong earthquakes [6,11]. The main reason for the serious disaster lied in that the buildings had poor anti-seismic properties. Since the reinforced steel bar is one of the most important material to insure the safety of building structures, the anti-seismic performances of building structures depend on the actual performances of the reinforcing steel bars under earthquakes. The LCF or ELCF performance is one of the important indicator of the anti-seismic performance which was put forward by researchers [12,13] through numerous experiments

Research & Reviews: Journal of Material Sciences
DOI: 10.4172/2321-6212.1000182
e-ISSN: 2321-6212
p-ISSN: 2347-2278

and investigations. However, since vast time and energy have to be spent on the fatigue experiments, the criterion of selecting the construction steel used to be established on the basis of the statistic strength of steels in the anti-seismic design [13]. Therefore, it is obviously dangerous that the whole distinction of the service conditions and failure pattern between the dynamic loading and static loading were ignored. As an indispensable factor for anti-seismic design, it is of great necessity to achieve a comprehensive and in-depth understanding of the ELCF behaviors of construction steels.

Recently, more and more investigations on LCF behavior of construction steels and structures have been carried out [14-16]. However, there are few reports about the research on the ELCF yet. The extremely large strain amplitude and relatively huge accumulated plastic strain during the ELCF could result in special plastic deformation bahaviour which causes unique changes in the cyclic hardening/softening behaviours during cyclic loading processes [4]. Another unique characteristic of ELCF different from other fatigue regimes is its fracture mode. The fatigue crack often starts from the surface during the LCF regime, while in the ELCF region, the fatigue crack probably originates from the interior of the specimen [17].

Moreover, Coffin-Manson [18,19] relationship was employed to establish the life prediction model and fit the LCF life prediction curve. Since little experimental data was obtained, ELCF life used to be predicted by the strain-life relationship of LCF life based on Coffin-Manson relationship. However, research results suggested that Coffin-Manson relationship often overestimated the ELCF life of some materials [20-22], although it may be applicable to other materials [10,23]. Undoubtedly, being overestimated of ELCF life would cause danger to building structures under strong earthquakes. Although Kanvinde and Deierlein [24] has researched the fatigue damage by contributing the effect of plastic internal void growth and coalescence in ELCF and developed a cyclic void growth model (CVGM) for ELCF life prediction showing fairly accurate results of predicting ELCF life, the CVGM is limited by some assumptions stated in the study. So far, researchers are not yet certain whether or not the Coffin-Manson law is applicable to the ELCF prediction [25], which makes ELCF life prediction unsolved problem in ELCF investigation. Due to these analyses, a comprehensive and in-depth understanding of the ELCF behaviours of earthquake resistant building steels was considered in this paper.

At present, HRB400 reinforcing steel bars were widely applied in the earthquake-prone areas. Its LCF properties have been investigated [14,15] before. However, so far there are no theoretical or experimental reports about its ELCF performances. Therefore, the ELCF behaviour of HRB400 reinforcing steel bars, such as the cyclic stress response, the life prediction model and damage mechanism, was investigated in the paper. The investigation would shed light on the estimation and improvement of the anti-seismic performances of the test material, and improve the research on the design and application of the steel structures under strong earthquakes. Meanwhile, this research would contribute to the improvement in the ELCF theory.

MATERIAL AND TESTING ARRANGEMENTS

Materials and Test Coupons

The chemical compositions, mechanical properties and micro-structure of the test material have been reported in previous research [15]. The extremely low fatigue tests were conducted on a servo-valve controlled electro-hydraulic testing machine from Shimadzu (model EHF-EM200k2-040) in ambient air at room temperature according to the standard [26]. The tests were run under uni-axial tension-compression loading with total strain control. Triangular waveform was employed for all the fatigue tests. The cyclic loading was started from the tensile side. The total strain was measured by a dynamic lateral extensometer which was attached to the minimum diameter of the specimen. The hourglass fatigue specimens with a minimum diameter of 8 mm were used **(Figure 1)**. Before fatigue testings, the specimens were machined by an NC machine, and the surfaces were polished by using grinding paste (W3.5) to remove scratches, finally as bright as a mirror.

Testing was carried out up to the fracture. Due to the little difference of fatigue life under each test condition, two specimens were tested for each experimental condition. The data in all figures is the average value of the measured results at each test condition. The number of cycles to failure for each specimen was recorded for the fatigue life. The response at half of the fatigue life was used to obtain cyclic stress-strain curves in this study.

Experimental Details and Procedures

In order to investigate the effect of strain amplitude, seven lateral strain amplitudes (±1.5%, ±2.0%, ±3.0%, ±4.0%, ±5.0%, ±6.0% and ±7.0%) with strain ratio of -1 and frequency of 1.0 Hz were applied. The axial strain amplitude ε was calculated by using the relation:

$$\varepsilon = (\sigma / E)(1 - 2\nu) + 2\varepsilon_d \quad (1)$$

Where σ is the stress amplitude, E is the elasticity modulus, ν is the elastic Poisson's ratio, and ε_d is the lateral strain amplitude.

Research & Reviews: Journal of Material Sciences
DOI: 10.4172/2321-6212.1000182
e-ISSN: 2321-6212
p-ISSN: 2347-2278

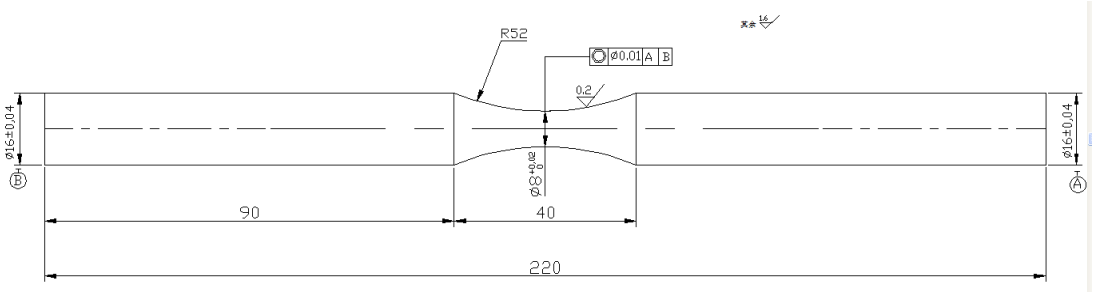

Figure 1. Geometry of specimen (unit: mm).

RESULTS AND DISCUSSION

Cyclic Stress Response

Figure 2 shows the cyclic stress response at different strain amplitudes of the test material, where **Figure 2b** shows magnified cyclic stress response curves under some special strain amplitudes in **Figure 2a**. The stress amplitudes increase significantly with increasing strain amplitudes, much higher than its nominal ultimate strength (604MPa). Different from the previous results of low cycle fatigue [15], the cyclic stress response under extremely low cycle fatigue depends on strain amplitude distinctly. In other words, it is suggested that the cyclic stress response may be controlled by the loading condition, which was also observed in Cu-Al alloys and high-Mn austenitic TRIP/TWIP alloys under ELCF [4,5]. The material showed significant cyclic stability at low strain amplitude of 3.131%, which is in accordance with the cyclic stress response at other lower strain amplitudes [15]. The reason lies in that the fatigue life at the amplitudes of below 3.131% belongs to the low cycle fatigue. However, the material showed slightly cyclic softening at high strain amplitude of 12.755%, while it showed secondary strain hardening at the medium amplitudes of 6.093% and 9.555%. That is to say, at the medium amplitudes the material showed rapid cyclic hardening at the initial stage of the fatigue life (below 10% fatigue life). After the initial hardening, the cyclic stress decreased at half-life and then increased again until the initiation of macro-crack where a rapid decrease in the cyclic stress occurred. This phenomenon of the secondary cyclic strain hardening has rarely been reported in the literature [27,28]. And the possible mechanisms for secondary cyclic strain hardening could be attributed to the dislocation multiplication, interaction between stacking faults and moving dislocations, which causes plastic deformation to become more difficult. The secondary cyclic strain hardening contributes to the improvement in the fatigue resistance [27,28].

Strain-Life Relationship

Tables 1 and 2 show the experimental results of the extremely low cycle fatigue and low cycle fatigue [15], respectively. The Poisson's ratio was 0.27 and the elastic modulus was 210GPa.

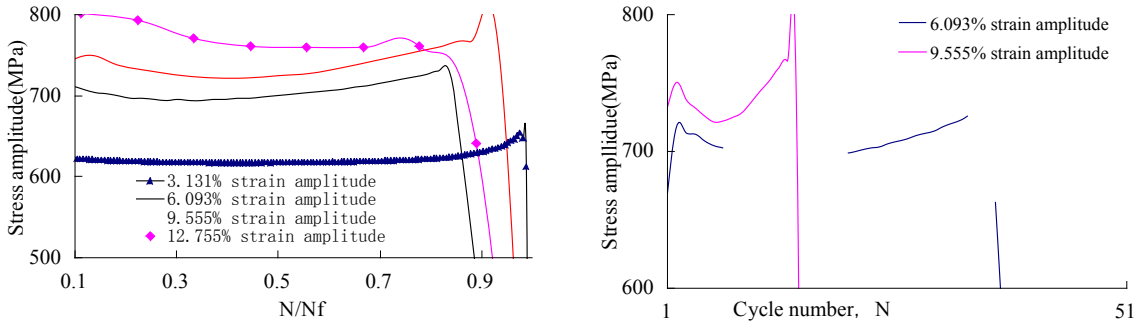

(a) At different strain amplitudes (b) Magnification of **Figure 2a**

Figure 2. Cyclic stress response.

Table 1. Results of ELCF tests.

Strain amplitude ε_d (%)	Elastic strain amplitude ε_{ea} (%)	Plastic strain amplitude ε_{pa} (%)	Stress amplitude σ_a (MPa)	$2N_f$	Actual lateral strain ε_d (%)
3.131	0.293	2.838	615	306	1.498
4.135	0.310	3.824	652	173	1.996
6.093	0.328	5.765	688	76	2.971
7.851	0.341	7.510	717	46	3.847
9.555	0.340	9.214	715	31	4.699
11.036	0.348	10.688	730	22	5.438
12.755	0.360	12.396	755	18	6.295

Research & Reviews: Journal of Material Sciences
DOI: 10.4172/2321-6212.1000182
e-ISSN: 2321-6212
p-ISSN: 2347-2278

Table 2. Results of LCF tests [15].

Strain amplitude ε_a (%)	Elastic strain amplitude ε_{ea} (%)	Plastic strain amplitude ε_{pa} (%)	Stress amplitude σ_a (MPa)	$2N_f$
0.5	0.199	0.301	450	2160
0.6	0.203	0.397	467	1838
0.7	0.210	0.490	486	1348
0.8	0.211	0.589	499	1082
0.9	0.222	0.678	517	922
1.0	0.238	0.757	527	674

Substituting the ELCF data, all data, LCF data and the cylindrical data in **Table 1** into the Coffin-Manson relationship [18,19], respectively, the corresponding strain-life relationships were given in **Table 3**.

Figure 3 shows the strain-life curves plotted according to the strain-life relationships in **Table 3**. As it can be seen in **Figure 3a**, the predicted life agreed well with the experimental data, which implied that the Coffin-Manson relationship was applicable to the entire ELCF life prediction. **Figure 3b** shows the strain-life curve obtained by fitting all the LCF and ELCF data, where the predicted life basically agreed with the experimental data except for the middle amplitudes (3.131% and 4.135%). The relative dispersion at middle amplitudes may be caused by the employment of the cylindrical specimens at low amplitudes in LCF. Hence, the experimental data did not agree so well with the fitting curve in **Figure 3b** as in **Figure 3a**. **Figure 3c** shows the strain-life curve fitted by all the LCF data. In **Figure 3c**, the predicted ELCF life was overestimated by the strain-life curve fitted by all the LCF data and the error increased with an increasing strain amplitude, which was in accordance with some other materials [20,21]. **Figure 3d** shows the strain-life curve fitted by all the LCF data of the cylindrical specimens. Similar to **Figure 3b** the predicted life basically agreed with the experimental data except for the middle amplitudes. However, the LCF data agreed with the fitted curve better in **Figure 3d** than in **Figure 3b**. It can also be seen from **Figure 3d** that at the same amplitude the LCF life of hourglass specimen was longer than that of cylindrical specimen, and the gap of life between the two kinds of specimens increased with the decreasing strain amplitudes. The reason for the longer life of hourglass specimens may lie in that it has better stability and smaller dangerous region and thus has longer life. It can be concluded from **Figure 3a-d** that Coffin-Manson relationship is applicable to the prediction of the LCF and ELCF life on the basis of ELCF experimental data. However, there is a large error in the ELCF life prediction only according to the strain-life relationship fitted by the LCF experimental data(except for the ELCF experimental data). The reason for the large error lies in that the life of hourglass specimen was generally longer than that of cylindrical specimen at the same strain amplitude, although buckling could be prevented effectively by the employment of the hourglass specimens under high cyclic loading in ELCF. That is to say, it is safer to predict the ELCF life of hourglass specimens with the LCF experimental data of the cylindrical specimens than that of both hourglass and cylindrical specimens. Moreover, it is dangerous to predict the ELCF life of hourglass specimens with the LCF experimental data of both hourglass and cylindrical specimens.

Table 3. Strain-life relationship based on Coffin-Manson.

Data sources	Strain-life relationship	Correlation coefficient	Corresponding figure
ELCF data in **Table 1**	$\varepsilon_{pa} = 0.534(2N_f)^{-0.513}$	-0.999	**Figure 3a**
All data in **Tables 1 and 2**	$\varepsilon_{pa} = 1.453(2N_f)^{-0.780}$	-0.987	**Figure 3b**
LCF* data in **Tables 1 and 2**	$\varepsilon_{pa} = 10.410(2N_f)^{-1.066}$	-0.977	**Figure 3c**
LCF* Data from cylindrical specimens in **Table 2**	$\varepsilon_{pa} = 1.312(2N_f)^{-0.779}$	-0.980	**Figure 3d**

*LCF data means experimental results of fatigue life more than 100 cycles, and ELCF data means experimental results of fatigue life less than 100 cycles.

Research & Reviews: Journal of Material Sciences
DOI: 10.4172/2321-6212.1000182
e-ISSN: 2321-6212
p-ISSN: 2347-2278

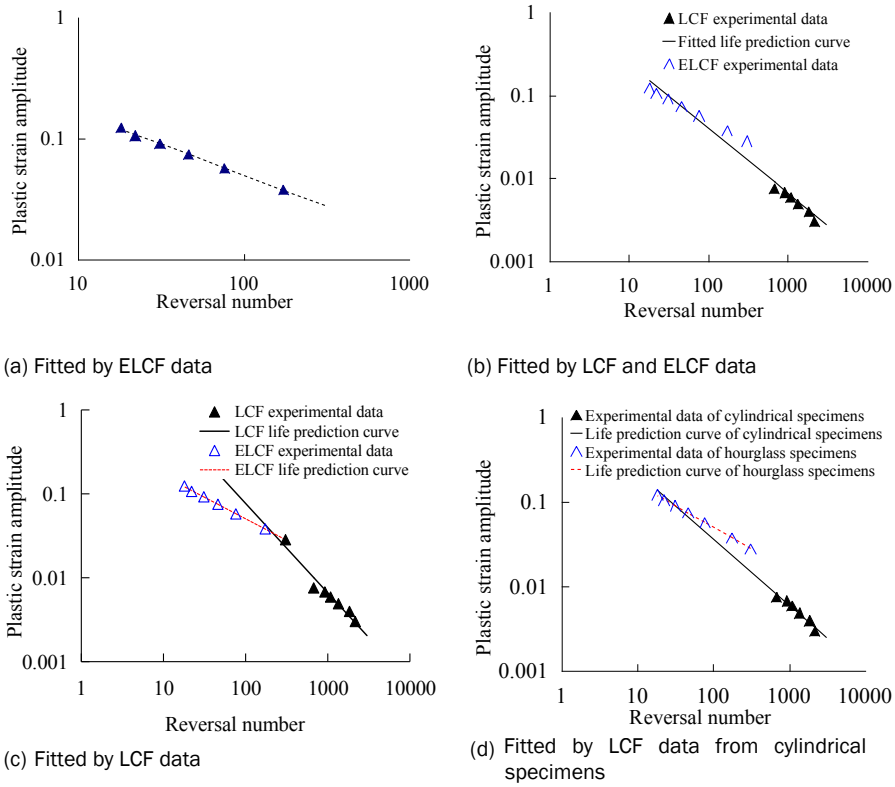

(a) Fitted by ELCF data

(b) Fitted by LCF and ELCF data

(c) Fitted by LCF data

(d) Fitted by LCF data from cylindrical specimens

Figure 3. Strain-life curves.

The Fracture Behaviors

Figure 4 shows the fracture surfaces of the sample fatigued at the strain amplitude of 7.851%. **Figure 4a** shows the fracture overall at an angle of about 45 degree to the loading axis, where there were several small crack initiation sites and a main crack initiation site. **Figure 4b** shows an amplified image of a small crack initiation site in **Figure 4a**, where it can be seen that cracks initiated at the surface. **Figure 4c** shows the morphology of the stable crack propagation region with wide fatigue striations located at the edge of the fracture, indicating a fast crack propagation speed. **Figure 4d** shows the dimples in the central region, where numerous fine dimples accumulated and an obvious inner crack with a length of about 0.3 mm existed. It is suggested that the damage of the test material in ELCF was caused by both the external and the internal cracks. And the final fracture region located in the central region was large, suggesting a fast fracture propagation speed, too.

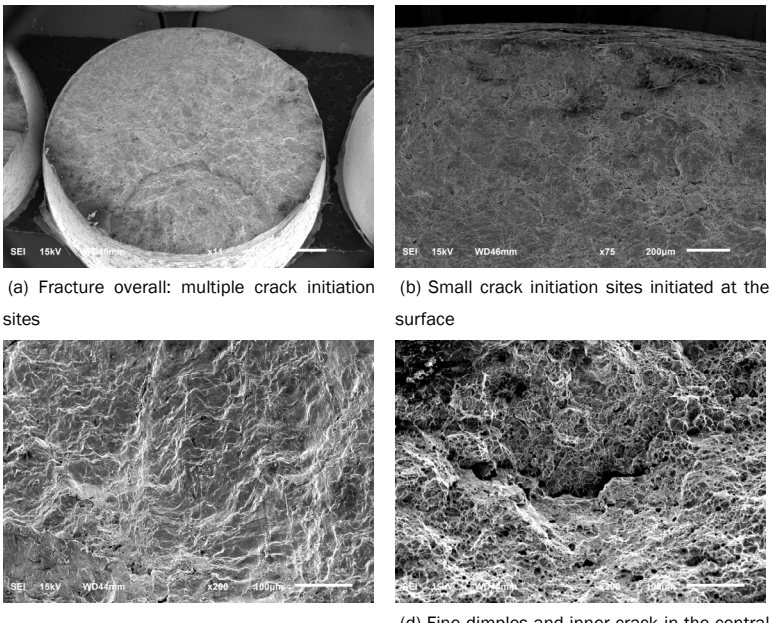

(a) Fracture overall: multiple crack initiation sites

(b) Small crack initiation sites initiated at the surface

(c) Striations in the propagation region

(d) Fine dimples and inner crack in the central region

Figure 4. Micro-graphs of fatigue fracture ($\Delta\varepsilon_t$=15.702%, N_f=23).

e-ISSN: 2321-6212
p-ISSN: 2347-2278

CONCLUSIONS

(1) The cyclic stress responses were dependent on the strain amplitudes. In ELCF, the test material exhibited slight cyclic softening at very high strain amplitudes, which was detrimental to improving the dynamic bearing capability. However, secondary strain hardening occurred at some strain amplitudes, which contributed to the improvement in the fatigue resistance.

(2) The variation of both LCF and ELCF life with plastic strain amplitude followed Coffin-Manson relationship. Hence, the ELCF life of the test material was predicted. However, it is dangerous to predict the ELCF life only according to the LCF data obtained from both the cylindrical and the hourglass specimens because the ELCF life would be overestimated. The research results provided the scientific basis to analyze the ELCF properties and life prediction of the test material.

(3) Several cracks initiated at the surface of the specimen, which results in multiple fatigue sites in ELCF. Then cracks propagated inward together, and exhibited a small propagation region. The final rupture regions of fractures in ELCF were larger than those in LCF. And contrary to LCF where the final fracture regions occurred on the edges of fractures, the final rupture regions existed in the central parts of fractures. The fractures in ELCF were caused by both the external and the internal damages. These investigations on the micro-phenomenon would not only shed light on the thorough comprehension of the micro-fracture mechanism but also promote to improve the anti-seismic properties of anti-seismic steels.

ACKNOWLEDGMENTS

Financial supports from the National Natural Science Foundation of China (No. 11327801, No. 1157205, No. 51301115, the Program for Changjiang Scholars and Innovative Research Team (IRT14R37), Key Science and Technology Support Program of Sichuan Province (2015JPT0001), the Key Science and Technology Support Program of Sichuan Province (2016GZ0294, the Project of Key Laboratory of Material Corrosion and Protection of Sichuan Province (2012CL10, 2016CL17, the Project of Sichuan Province Department of Education (16ZB0255, 13ZA0129, the Project of Key Lab in Sichuan Colleges on Industry Process Equipments and Control Engineering (GK201205, GK201501)and the Talent Introduction Project of Sichuan University of Science & Engineering (2015RC34) are acknowledged.

REFERENCES

1. Tao C. Extremely Low Cycle Fatigue Assessment of Thick-Walled Steel Piers. PhD Dissertation, Nagoya University 2007.
2. Wei YB, et al. Several problems on extra low cycle fatigue fracture design, J Gansu Industrial Univ 1998;24:109-112.
3. Zhao XC. Research on fracture properties of Q235 under the extra low cycle conditions. PhD Dissertation, Lanzhou University of Technology 2007.
4. Liu R, et al. Extremely-low-cycle fatigue behaviors of Cu and Cu-Al alloys: Damage mechanisms and life prediction. Acta Mater 2015;83:341-356.
5. Shao CW, et al. Low-cycle and extremely-low-cycle fatigue behaviors of high-Mn austenitic TRIP/TWIP alloys: Property evaluation, damage mechanisms and life prediction. Acta Mater 2016;103:781-795.
6. Tong LW, et al. Experimental and numerical investigations on extremely-low-cycle fatigue fracture behavior of steel welded joints, J Constr Steel Res 2016;119:98-112.
7. Pereira JCR, et al. Ultra low-cycle fatigue behaviour of a structural steel. Eng Struct 2014;60:214-222.
8. Xu LY, et al. Cyclic hardening and softening behavior of the low yield point steel BLY160: Experimental response and constitutive modeling. Int J Plast 2016;78:44-63.
9. Nip KH, et al. Extremely low cycle fatigue tests on structural carbon steel and stainless steel. J Constr Steel Res 2010;66:96-110.
10. Masayuki K. Fatigue properties of 316 stainless steel and its failure due to internal cracks in low-cycle and extremely low-cycle fatigue regimes. Int J Fatigue 2010;32:1081-1089.
11. Kang L and Ge H. Predicting ductile crack initiation of steel bridge structures due to extremely low-cycle fatigue using local and non-local models. J Earthq Eng 2013;17:323-349.
12. Sheng GM and Gong SH. Investigation of low cycle fatigue behaviour of building structural steels under earthquake loading. Acta Metall Sin-Engl 1997;10:51-55.
13. Gong SH and Sheng GM. Studies on steel in anti-seismic design. Earthquake Resistant Eng 1995;37-42.
14. Qin B, et al. Analysis on High strain low cycle fatigue properties of 20MnSiVHRB400 reinforced steel bars, J Chongqing Univ 2003;26:93-96.
15. Luo YR, et al. Low cycle fatigue properties of Anti-seismic steel HRB400 Reinforcing Steel Bars. J Iron Steel Res 2015;27:35-39.
16. Luo YR, et al. Energy-based prediction of low cycle fatigue life of high-strength structural steel. J Iron Steel Res Int 2012;19:47-53.

e-ISSN: 2321-6212
p-ISSN: 2347-2278

17. Nip KH, et al. Cyclic testing and numerical modelling of carbon steel and stainless steel tubular bracing members. Eng Struct 2010;32:424-441.

18. Coffin LF. A study of the effects of cyclic thermal stresses on a ductile metal. Trans ASME 1954;76:931-950.

19. Manson SS. Behavior of materials under conditions of thermal stress. Tech Rep Arch Image Library 1953;7:661-665.

20. Tateishi K, et al. A prediction model for extremely low cycle fatigue strength of structural steel. Int J Fatigue 2007;29:887-896.

21. Kuroda M. Extremely low cycle fatigue life prediction based on a new cumulative fatigue damage model. Int J Fatigue 2002;24:699-703.

22. Xue L. A unified expression for low cycle fatigue and extremely low cycle fatigue and its implication for monotonic loading. Int J Fatigue 2008;30:1691-1698.

23. Shimada K, et al. The applicability of the Manson-Coffin law and Miner's law to extremely low cycle fatigue, J Japan Soc Mech Eng 1987;53:1178-1185.

24. Kanvinde AM and Deierlein GG. Cyclic void growth model to assess ductile fracture initiation in structural steels due to ultra-low cycle fatigue. J Eng Mech-ASCE 2007;133:701-712.

25. Algarni M, et al. A unified material model for multiaxial ductile fracture and extremely low cycle fatigue of Inconel 718. Int J Fatigue 2017;96:162-177.

26. GB/T15248-2008. The Test Method for Axial Loading Constant-amplitude Low-cycle Fatigue of Metallic Materials, China Standards Institution 2008.

27. Chai GC, et al. Low and High Cycle Fatigue Behavior of Nickel-base Alloy at High Temperatures. Procedia Eng 2013;55:671-676.

28. Chai GC, et al. Cyclic deformation behaviour of a nickel base alloy at elevated temperature. J Mater Sci 2004;39:2689-2697.